RSC Advances

ROYAL SOCIETY OF CHEMISTRY

www.rsc.org/advances

Graphical Abstract:

Three new Cu(II), Ru(II), and Pt(II) compounds of anthracene-containing tripodal ligand were synthesized and characterized.Their crystal structures of compounds were determined by single-crystal X-ray diffraction method and their antimicrobial activities were investigated.

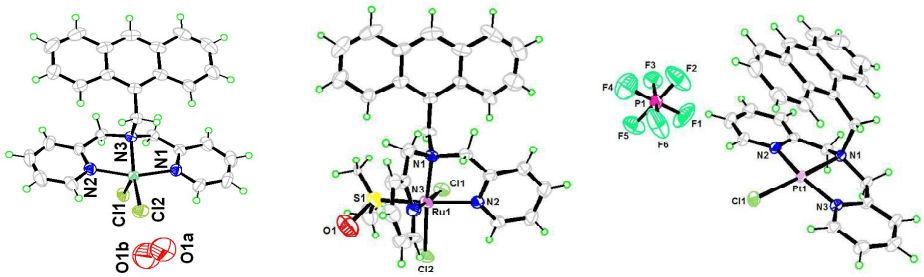

Journal Name

RSCPublishing

ARTICLE

Syntheses, crystal structures and antimicrobial activities of Cu(II), Ru(II), and Pt(II) compounds with anthracene-containing tripodal ligand

Cite this: DOI: 10.1039/x0xx00000x

Zeli Yuan[a,b],Xiaoming Sheng[a] and Jiandong Huang*[a]

Received 00th January 2014,
Accepted 00th January 2014

DOI: 10.1039/x0xx00000x

www.rsc.org/

Three coordination polymers based on a tridentate N3-coordinated anthracene-containing tripodal ligand, 9-[(2,2′-dipicolylamino)methyl]anthracene (ADPA), namely $[Cu(ADPA)Cl_2]\cdot H_2O$ (**1**), $[Ru(ADPA)Cl_2DMSO]\cdot 4CH_3OH\cdot 2H_2O$ (**2**), and $[Pt(ADPA)Cl]PF_6\cdot DMSO\cdot 2CH_3OH\cdot H_2O$ (**3**), were synthesized and characterized using elemental analysis, ^1H NMR, ^{13}C NMR, FT-IR, and UV-vis spectroscopies, HRMS, and single-crystal XRD. X-ray structural analysis showed that the three compounds have mononuclear, 0D structures, which are further connected by hydrogen bonds into 3D supramolecular architectures. The antimicrobial activities of ADPA and compounds **1**–**3** were evaluated based on the minimum inhibitory concentration and minimum bactericidal concentration. The results showed that compounds **1**–**3** exhibit significant activities against Gram-positive bacteria (*Staphylococcus aureus*), and the Ru(II) and Pt(II) compounds have moderate antifungal activities (*Candida albicans*).

Introduction

Antimicrobial resistance is rapid becoming a global concern, with a fast increase in multidrug-resistant bacteria.[1] The discovery of novel active compounds against new targets is therefore urgently needed to deal with the worrying problem of microbial resistance to antibiotics.[2]

The use of metal ions in therapeutic agents is known to accelerate drug action, and their efficacy is enhanced by coordination with metal ions.[3a] There is much evidence that compounds of metals such as Cu(II), Ru(II), and Pt(II) with high positive charges are potential novel types of broad-spectrum antibacterial compounds, and some compounds have shown potential applications as antimicrobial agents.[3] These systems bind tightly to either DNA or RNA, and some can hydrolyze the phosphodiester bonds of nucleotides.[4] It has been shown in some cases that metal compounds containing organic drugs as ligands can overcome the resistance developed by bacteria to the organic compounds alone.[5] In recent decades, much effort has therefore been devoted to the development of various types of supporting ligands to generate metal compounds as potential chemotherapeutic or diagnostic agents.

Cu(II) is a biometal; its compounds have low toxicities and some of them perform important cellular functions such as neurotransmission and cellular respiration.[6] The Cu(II) ion has relatively strong Lewis acidity, high nucleobase affinity, and efficient DNA cleavage activity. Recently, Cu(II) compounds with N-donor ligands have shown numerous biological activities such as antitumor and antibacterial activities.[7] Ru compounds of various types figure prominently among metallodrugs. The classic Ru(III) compounds NAMI-A and KP1019 have successfully passed phase I clinical trials,[8] and organometallic Ru(II)–arene compounds are a rapidly developing new class of metallodrugs.[9] Pt compounds are among the most promising drugs in cancer chemotherapy, and many Pt(II) compounds with wide ranges of biological activities such as antimicrobial, anti-inflammatory, and antiviral activities have also been reported.[10]

The above observations suggest that new transition-metal compounds with improved antibacterial activities could be developed. Anthracenyl rings play a major role in extending the pharmacological properties of synthesized drugs.[11] In view of the diverse chelating behavior of dipicolylamine [*N*,*N*-bis(2-pyridylmethyl)amine, DPA],[12] and the biological importance of Cu(II), Ru(II), and Pt(II) compounds, and their interesting structural properties, it was considered worthwhile to synthesize and characterize some new Cu(II), Ru(II), and Pt(II)

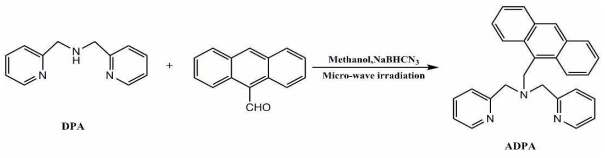

Scheme 1 Synthesis of ligand(ADPA).

compounds with an anthracene-containing tripodal ligand.

In this study, we designed and successfully synthesized three new Cu(II), Ru(II) and Pt(II) compounds, **1**–**3**, which have a DPA ligand with a pendant anthracenyl moiety, as a typical DNA intercalator binder (Scheme 1). The crystal structures of **1**–**3** were determined using single-crystal XRD. Antimicrobial experiments showed that the activities of **1**–**3** against Gram-positive bacteria (*Staphylococcus aureus*, CGMCC-1.1477) were stronger than that of the ligand, suggesting that these three compounds could be developed as new antimicrobial agents. The Ru(II) and Pt(II) compounds, *i.e.*, **2** and **3**, had moderate antifungal activities (*Candida albicans*, ATCC-10213).

Experimental

Materials and methods

All chemicals and reagents obtained from commercial sources were AR grade and used without further purification. DPA, *cis*-$RuCl_2(DMSO)_4$, and *cis*-$PtCl_2(DMSO)_4$ were synthesized using previously reported procedures.[13] ^1H and ^{13}C NMR spectra were recorded, using an Agilent 400 DD2 spectrometer, in DMSO-d_6 or $CDCl_3$, with tetramethylsilane as the internal reference. H RMS were recorded using a time-of-flight Micromass LCT PremierXE spectrometer. UV-vis absorption spectra were recorded using a Cary 50 spectrophotometer. Elemental (C, H, N) analyses were performed using a Vario EL III elemental analyzer. IR spectra were recorded, using KBr pellets, with a Vary FT-IR 1000 spectrophotometer in the range 400 – 4000 cm^{-1}. Powder XRD patterns of crushed single crystals were recorded in the 2θ range 5–55° using Mo Kα radiation. Thermogravimetric experiments were performed using a TGA/NETZSCH STA-449C instrument, in the range 30–800 °C (heating rate 10 °C/min, N_2 stream).

Synthesis of 9-[(2,2′-dipicolyl-amino)methyl]anthracene(ADPA)

9-Anthraldehyde (1 mmol) and DPA (1 mmol) in MeOH (5 mL) in a round-bottomed flask were irradiated at 300 W at 60 °C for 15 min. $NaBH_3CN$ (1.2 mmol) was added and the mixture was irradiated of 300 W at 60 °C for 30 min. Basic workup using a saturated aqueous sodium carbonate solution and subsequent extraction using CH_2Cl_2 was performed. The combined organic layers were washed with water and brine, followed by drying over $MgSO_4$. After removal of the solvent *in vacuo*, the residue was washed with a small amount of MeOH, followed by recrystallization from THF–AcOEt to give the ligand as a yellow powder. The isolated yield was 0.34 g (89%). mp147–148 °C. ^1H NMR (400 MHz, $CDCl_3$) δ: 3.88 (4H, s), 4.66 (2H, s), 7.07–7.09 (2H, dd, J = 5.1, 8.4 Hz), 7.30–7.31 (2H, d, J = 8.4 Hz), 7.40–7.47 (4H, m), 7.54–7.58 (2H, ddd, J = 1.8, 8.6, 7.8 Hz), 7.92–7.94 (2H, d, J = 8.9 Hz), 8.34–8.39 (3H, m, J = 7.1 Hz), 8.49–8.48 (2H, d, J = 7.6 Hz).^{13}C NMR(100 MHz, $CDCl_3$) δ: 159.60, 148.70, 136.21, 131.46, 131.33, 128.88, 127.63, 125.58, 125.05, 124.79, 123.57, 121.98, 60.57, 50.81. HRMS (ESMS) calc. for $C_{27}H_{23}N_3$ $(M + H)^+$: 390.1970, found m/z: 390.1978. Calc. for $C_{27}H_{23}N_3$: C 83.26, H 5.95, N 10.79, found: C 83.22, H 6.01, N 10.69. FT-IR (cm^{-1}) 3050, 2929, 2882, 2813, 1588, 1567, 1472, 1433, 885, 734. UV-vis (acetonitrile, 1.0×10^{-6} mol/L, λ_{max}/nm) 387, 367, 349.

Synthesis of $[Cu(ADPA)Cl_2]\cdot H_2O$ (1)

An ethanolic solution of $CuCl_2\cdot 2H_2O$ (0.17 g, 1.0 mmol) was added to a hot ethanolic solution of ADPA (0.39 g, 1.0 mmol), with constant stirring with a magnetic stirrer. The green solution was stirred for an additional hour with heating. On slow evaporation, the desired compound separated out as green flakes; the solid was recovered by filtration, washed with cold ethanol and diethyl ether, and dried over anhydrous $CaCl_2$. The isolated yield was 0.46 g (78%). A single crystal for XRD was again obtained via vapor diffusion of diethyl ether into a concentrated methanol solution over 3 d at room temperature. Anal. Calc. For $C_{27}H_{23}N_3Cl_2Cu\cdot H_2O$: C 59.84, H 4.65, N 7.75; found: C 59.88, H 4.68, N 7.63; H RMS (ESMS) calculated for $C_{27}H_{23}N_3Cl_2Cu(M + H)^+$: 522.0565, found m/z:522.0561; FT-IR: 3433, 3070, 3027, 2966, 2921, 2871, 1606, 1474, 1435, 1277, 748, 473; UV-vis (acetonitrile, 1.0×10^{-6} mol·L^{-1}, λ_{max}/nm) 289, 358, 376, 396.

Synthesis of $[Ru(ADPA)Cl_2DMSO]\cdot 4CH_3OH\cdot H_2O$ (2)

Solid *cis*-$[RuCl_2(DMSO)_4]$ (0.42 g, 1 mmol) was added to a degassed solution of ADPA (0.39 g, 1 mmol) and NEt_3 (0.31 g, 3 mmol) in MeOH (10 mL). The mixture was refluxed for 4 h under N_2. The yellow precipitate was recovered by filtration, washed with MeOH and diethyl ether, and dried. The isolated yield was 0.46 g (70%). A single crystal for XRD was obtained *via* vapor diffusion of diethyl ether into a concentrated acetonitrile solution of the compound over 3 d at room temperature. ^1H NMR(400 MHz, DMSO-d_6) δ: 3.33(s, 12H), 3.49 (s, 6H), 4.49-4.53(d, J=15.1 Hz, 2H), 4.70(s, 2H), 5.29-5.35(d, J=15.1 Hz, 2H), 7.43-7.46(t, J=6.5 Hz, 2H), 7.61-7.63 (d, J=7.7 Hz, 2H), 7.72 -7.75(d, J=9.3 Hz, 1H),7.90-7.94 (m, 3H), 8.13-8.16(t, J=7.6 Hz, 1H), 8.24-8.26(d, J=7.9 Hz, 1H), 8.29(s, 1H), 8.37-8.40(m, 2H), 8.43 -8.45 (d, J=7.9 Hz, 1H), 8.91-8.92(d, J=5.5 Hz, 2H); ^{13}C NMR(100 MHz, DMSO-d_6) δ: 55.33, 63.31, 120.74, 123.69, 124.98, 127.20, 132.13, 135.43, 137.19, 164.10; Calcd for $C_{29}H_{29}N_3OCl_2SRu\cdot 4CH_3OH\cdot H_2O$: C, 50.44; H, 6.03; N,5.35. Found: C, 49.82; H, 5.55; N, 5.57 ; H RMS (ESMS) calculated for $C_{29}H_{29}N_3OCl_2SRu$ $(M)^+$: 639.0452; found m/z: 639.0444; FT-IR: 3463, 3085, 3018, 2967, 2923, 1601, 1564, 1473, 1436, 1149, 1064, 745, 435; UV-vis(acetonitrile, 1.0×10^{-6} mol/L, λ_{max}/nm) 351, 369, 389.

Synthesis of $[Pt(ADPA)Cl]PF_6\cdot DMSO\cdot 2CH_3OH$(3)

Solid *cis*-$[PtCl_2(DMSO)_4]$ (0.58 g, 1 mmol) was added to a degassed solution of ADPA (0.39 g, 1 mmol) and NEt_3 (0.31 g, 3 mmol) in MeOH (10 mL). The mixture was refluxed for 4 h under N_2, and a 5 mL aliquot of a saturated solution of NH_4PF_6 was added. The solution was placed in a freezer overnight to aid precipitation of the product. The white precipitate was recovered by filtration, washed with MeOH and diethyl ether, and dried. The isolated yield was 0.78 g (83%). A single crystal for XRD was obtained *via* vapor diffusion of diethyl ether into a concentrated acetonitrile solution of the compound over 7 d at room temperature. ^1H NMR(400 MHz, DMSO-d_6) □δ: 2.52(s,

6H), 3.35(s, 6H), 5.09-5.13 (d, *J*=15.5 Hz, 4H), 5.40-5.44(d, *J*=15.8 Hz, 2H), 7.09-7.13(d, *J*=6.6 Hz, 2H), 7.41-7.43(d, *J*=7.8 Hz, 2H), 7.75-7.79(td, *J*=7.8, 1.5 Hz, 2H), 7.98-8.02(t, *J*=8.1 Hz, 2H), 8.08-8.12(t, *J*=7.6 Hz, 1H), 8.15-8.17(d, *J*=9.0 Hz, 1H), 8.28-8.34(dd, *J*=16.5, 7.9 Hz, 4H), 8.37-8.39(d, *J*=7.5 Hz, 1H), 8.53-8.55 (d, *J*=7.9 Hz, 1H), 8.89-8.91(d, *J*=9.3 Hz, 1H); ^{13}C NMR(100 MHz, DMSO-d_6) δ: 40.52, 63.48, 68.37, 122.88, 123.27, 124.19, 125.95, 126.58, 126.93, 128.31, 130.15, 131.73, 132.07, 140.13, 148.32, 165.11; Anal. Calcd for $C_{27}H_{23}N_3ClPtPF_6$·DMSO·2CH_3OH: C, 48.85; H, 4.89; N, 5.51; Found: C, 48.69; H, 4.65; N, 5.77; H RMS (ESMS) calculated for $C_{27}H_{23}N_3ClPt(M)^+$: 619.1228; found m/z: 619.1208; FT-IR: 3463, 3085, 3018, 2967, 2923, 1601, 1564, 1473, 1436, 1144, 1064, 745, 435. UV-vis(acetonitrile, 1.0×10^{-6} mol/L, λ_{max}/nm) 363, 381, 401.

Crystal Structure Determination

Single-crystal XRD data were collected using a Rigaku diffractometer with a mercury charge-coupled device area detector (Mo Kα; λ = 0.71073 Å) at room temperature. Empirical absorption corrections were applied to the data using the Crystal Clear program.[14] The structure was solved by the direct method and refined by the full-matrix least-squares method on F^2 using the SHELXTL-97 program.[15] Metal atoms were located from *E*-maps and other non-hydrogen atoms were located in successive difference Fourier syntheses. All non-hydrogen atoms were refined anisotropically. The organic hydrogen atoms were positioned geometrically, and those in water molecules were located using the difference Fourier method and refined freely. PLATON/SQUEEZE was used to remove the heavily disordered water molecules, and the final formulas of **1** and **2** were determined based on the TGA results (Figs. S17† and S18†). Crystallographic data and other pertinent information for **1**–**3** are summarized in Table S1†. Selected bond distances and angles are listed in Tables S2–S4†. Bond lengths and angles of hydrogen bonds are listed in Tables S5† and S6†.

In vitro antimicrobial assay

The antimicrobial activities of ADPA and compounds **1**–**3** were tested against a Gram-positive strain, *S. aureus* CGMCC-1.1477, a Gram-negative strain, *Escherichia coli* ATTC-25922, and a fungal strain *C. albicans* ATCC-10213; these were obtained from the Division of Microbiology, Department of Basic Medicine, Zunyi Medical University of China. Suspensions in sterile peptone water from 24 h cultures of the microorganisms were adjusted to 0.5 McFarland. Muller–Hinton petri dishes of 90 mm were inoculated using these suspensions. Paper disks (diameter 6 mm) containing 10 μL of the substance to be tested (at a concentration of 2048 μg/mL in DMSO) were placed in a circular pattern in each inoculated plate. The plates were incubated at 37 °C for 24 h. The results were read by measuring the diameters of the inhibition zones generated by the tested substances, using a ruler. The minimum inhibitory concentration (MIC, μg/mL) and minimum bactericidal concentration (MBC, μg/mL) were determined using the serial dilution in liquid broth method.[16] The materials used were 96-well plates, suspensions of microorganism (0.5 McFarland), Muller–Hinton broth (Merck), and solutions of the substances to be tested (2048 μg/mL in DMSO). The following concentrations of the substances to be tested were obtained in the 96-well plates: 1024, 512, 256, 128, 64, 32, 16, 8, 4, and 2 μg/mL. After incubation at 37 °C for 18–24 h, the MIC for each tested substance was determined by macroscopic observation of the microbial growth. The MIC corresponds to the well with the lowest concentration of the tested substance where microbial growth was clearly inhibited.

Results and Discussion

Synthesis

ADPA was synthesized according to our previous work[17] by reductive amination coupling, using a monohydride source as the reducing agent, under microwave irradiation (Scheme 1). Despite the steric bulk of the aldehydic groups, this synthetic approach is more efficient than traditional methods[18] using microwave irradiation as the heat source. Compound **1** was obtained by direct reaction of $CuCl_2$ with ADPA in MeOH solution, in satisfactory yield (78%). Compound **2**, which contains an S-bound DMSO molecule, was synthesized by the reaction of ADPA with *cis*-[$RuCl_2(DMSO)_4$] in MeOH in the presence of NEt_3 as a base. We examined various reaction conditions, and found that for formation of **2**, it was necessary to use MeOH as the solvent and NEt_3 as the base. Compound **2** was not obtained from the reaction in acetonitrile, MeOH, or ethanol with NaH as the base. This is because reduction of the Ru(II) center is achieved by a combination of MeOH and NEt_3.[19] However, the mechanism is not clear at this point. Compound **3** was obtained using the same procedure as for compound **2**, but with NH_4PF_6 as a precipitator.

Characterisation and spectroscopic properties

ADPA and **1**–**3** gave satisfactory C, H, and N analyses; the results showed that the compositions of **1**–**3** were [Cu(ADPA)Cl_2]·1.5H_2O,[Ru(ADPA)Cl_2DMSO]·4CH_3OH·H_2O, and [Pt(ADPA)Cl]PF_6·DMSO·2CH_3OH, respectively.

The ^{1}H NMR spectra of **2** and **3** (Fig. S2† and S3†) in DMSO-d_6 enabled the specific binding mode of ADPA to be deduced. The aromatic portion of the spectrum showed that the two pyridyl units were equivalent and shifted downfield with respect to the free ligand, suggesting that both pyridyl units are coordinated to the Ru(II) and Pt(II) centers. The methylene linker units also showed significant deviations from the chemical shifts of the corresponding free ligand. The anthracenyl methylene linker was observed as a singlet at 5.43 ppm. Two sets of resonances were assigned to the diastereotopic protons of the pyridyl methylene linkers; each integrated to two protons and each had a coupling constant of *ca.* 15 Hz, confirming geminal two-bond coupling. The methyl proton signals of DMSO deserve special attention. The spectrum of **2** shows one DMSO signal, *i.e.*, a singlet at 3.49 ppm. This is assigned to coordinated DMSO.[19] Integration gave 6H for the protons of coordinated DMSO in **2**, as required by the stoichiometry and confirmed by XRD. In the spectrum of **3**, one DMSO signal is also observed, a singlet at 2.52 ppm, but the integral of the signal corresponds to 12H; therefore the ratio of compound molecules to noncoordinated DMSO is 1:1, in

accordance with the elemental analysis. The spectra of compounds **2** and **3** also show singlets at 3.33 and 3.35 ppm, assigned to CH_3OH.

The ^{13}C NMR spectra of ADPA and **2** and **3** are shown in Fig. S5† and S6†. The assignments are in agreement with the data for other chelate compounds and for Pt(II) or Ru(II) sulfoxide compounds.[19] The signals for coordinated DMSO appear in the spectrum of **2** at 44.08 and 43.32 ppm (Fig. S5†). Such signals are not observed in the spectrum of ADPA. In the spectrum of **3**, the solvent (DMSO) signal is expanded, with an additional signal at 40.52 ppm, closely situated to the lowest-frequency component of the septet (Fig. S6†). The signal corresponds to free (non-coordinated) DMSO, and, in the case of the Pt(II) compound **3**, arises from DMSO solvate molecules. The intensity of the DMSO-d_6 signal should be distributed over seven lines and, under the given conditions, such a signal could easily be masked by noise.

The H RMS of **1** had a parent ion peak at *m*/*z* 522.0561 (Fig. S8†), corresponding to the monoprotonated form. However, the dominant features in the HR ESMS of **2** and **3** (Fig. S9† and S10†), namely cationic fragment peaks at *m*/*z* 639.0444 and 619.1208 for **2** and **3**, respectively, were associated with the intermediate compounds $[Ru(ADPA)Cl_2DMSO]^+$ and $[Pt(ADPA)Cl]^+$. This is because ionization induced loss of the DMSO, MeOH, and PF_6^- ligands, to form cationic fragments, and is a common observation in the mass spectra of species of this type.

The FT-IR spectra of ADPA and **1**, **2**, and **3** are shown in Fig. S12–S14†. It is known that the $\upsilon_{(SO)}$ stretching band of sulfur-coordinated DMSO appears at a higher frequency than that of free DMSO; the typical ranges for Ru(II) and Pt(II) compounds are 1120–1170 cm^{-1},[21] although a value of 1195 cm^{-1} has also been reported.[22] The band at 1144 cm^{-1} in the spectrum of **2** could be assigned to the $\upsilon_{(SO)}$ vibration of sulfur-coordinated DMSO. However, this assignment is uncertain, because in the spectrum of the free ligand there is also a band in this interval. In addition, in the FT-IR spectrum of solid-state free DMSO, the $\upsilon_{(SO)}$ vibrations usually appear at 1050–1080 cm^{-1},[23]so the band at 1064 cm^{-1} could be assigned to $\upsilon_{(SO)}$ vibrations of the noncoordinated (solvate) DMSO in **3**. Moreover, the bands at 473, 424, and 435 cm^{-1}, which have no corresponding bands in the spectrum of the free ligand, could be ascribed to metal–nitrogen stretching vibrations for **1**–**3**,[24] respectively.

The UV-visible spectra of ADPA and **1**–**3** are shown in Fig. S15†. The absorption spectra of the compounds closely resemble those of the free ligand. The spectra of **1**–**3** are dominated by ligand-based π–π* transitions at 334 to 401 nm.[25] The higher-energy transitions are caused by pyridyl units, and the lower-energy transitions, for example at 349 nm, originate from anthracyl. This is in contrast to bisimine compounds of Re^+, which tend to be brightly colored because of metal-to-ligand charge-transfer transitions at 360–420 nm.[26] In the ligand spectrum, there is a weak absorption band at 333 nm from a charge-transfer transition and a strong absorption band at 285 nm, assigned to π–π* transitions. The absorption band at about 285 nm was blue shifted in the case of **1**, and the absorption intensity increased compared with that of the ligand. The blue shift of the band in **1** indicates that coordination decreases the delocalization of p electrons, resulting in an increase in the energy of the π–π* transition.[26]

XRD patterns and thermal stability analysis

Powder XRD was performed to test the purities of compounds **1** and **3** (Fig. S16† and S17†). The experimental results match the simulated XRD patterns well, indicating phase purity of the synthesized samples.

The TGA curve of **1** shows the loss of 1.5 guest water molecules at 49–100 °C (observed 3.94%, calc. 4.05%; Fig. S18†). The TGA curve of **2** indicates that a guest water molecule is gradually released at 30–230 °C (observed 2.59%, calc. 2.74%; Fig. S19†). However, **3** shows a weight loss of 10.72% at 47–200 °C, attributed to the loss of noncoordinated DMSO molecules (calc. 11.18%; Fig. S20†).[27]

Description of crystal structure

Single-crystal XRD analysis showed that compound **1** crystallizes in the monoclinic P21/n system, and its asymmetric unit contains one Cu(II) ion, one ADPA molecule, and two coordinated chloride ions (Fig. 1). The mononuclear Cu(II) was pentacoordinated, in a distorted square-pyramid, with two N atoms from two pyridine rings, with bond lengths Cu–N(1) 2.005(3) Å and Cu–N(2) 2.008(3) Å, one N atom from the amine nitrogen, with bond length Cu–N(3) 2.091(3) Å, and two chloride ions (Table S1†). The axial Cu–Cl(1) distance [2.2572(13) Å] is longer than the Cu–Cl(2) distance [2.4855(15) Å]; this difference originates from the Jahn–Teller distortion typical of a Cu(II) complex with a d9 electronic configuration electronic configuration.

In addition, there are two types of hydrogen-bonding interactions in **1**.

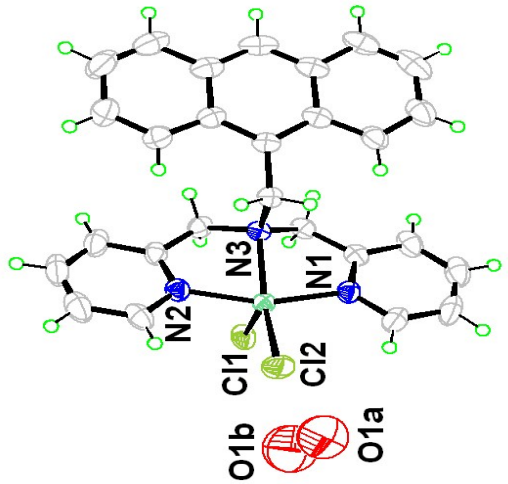

Fig. 1 Molecular structure of **1** with thermal ellipsoids at 45% probability.

The first is intramolecular hydrogen bonding between the carbon atoms in the pyridine ring and Cl(2) atoms [C(21)–H(21A)···Cl(2) = 3.2901 Å, ∠C(21)–H(21A)···Cl(2) 19° and C(27)–H(27A)···Cl(2) = 3.3009 Å, ∠C(27)–H(27A)···Cl(2) = 120°] (Table S5†). Intramolecular hydrogen bonding enhances the stability of molecular structures. The second type is the intermolecular hydrogen bonding interactions also between the carbon atoms pyridine ring and the Cl(1) atoms [C(20)-H(20A)···Cl(1) = 3.5062 A˚, ∠C(20)-H(20A)···Cl(1) = 147º and C(26)-H(26A)···Cl(1) = 3.4745 A˚, ∠C(26)-H(26 A)···Cl(1) = 141º], to extend the adjacent molecular structures into a 3D-supramolecular architecture (Fig. 2).

Compound **2** crystallizes in the trigonal space group of R-3 and its asymmetric unit contains one Ru(II) ion, one ADPA, two coordinated chloride ions and one coordinated DMSO molecule (Fig. 3). The Ru (II) center was six-coordinated by two N atoms from two pyridine rings with the Ru–N bond lengths of Ru–N(2) 2.097(3) Å and Ru–N(3) 2.077(3) Å, one N atom from the amine nitrogen with Ru–N bond lengths of and Ru–N(1) 2.142(3) Å, one S atom from the DMSO molecule with the Ru-S bond lengths of 2.2284(12) Å and two

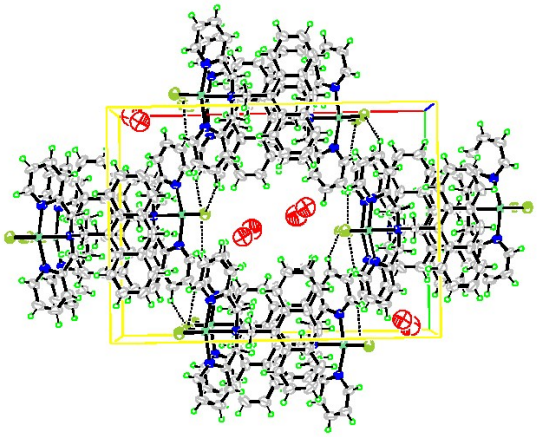

Fig. 2 Hydrogen-bonding interactions in **1** (*c*-axis projection).

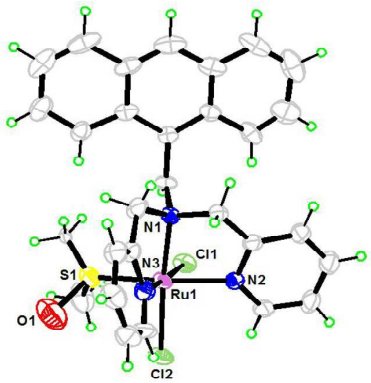

Fig. 3 Molecular structure of **2** with thermal ellipsoids at 45% probability.

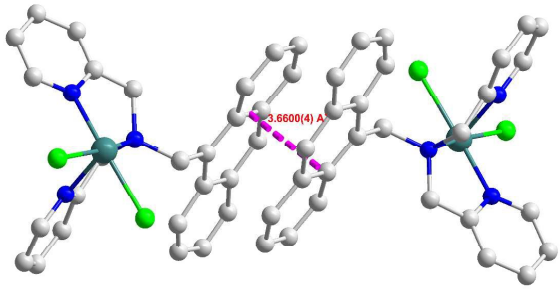

Fig. 4 View of π–π interactions between anthracene rings in **2**.

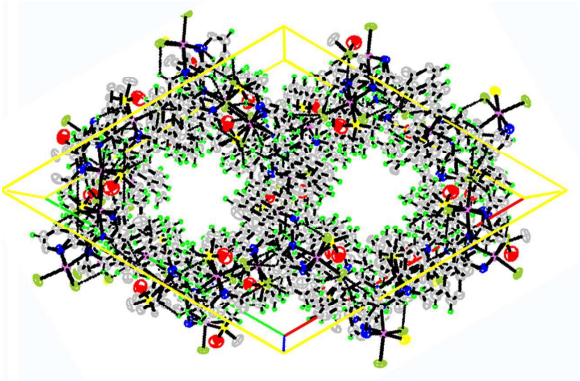

Fig. 5 Hydrogen-bonding interaction in **2** (*c*-axis projection).

coordinated chloride ions with the Ru–Cl bond lengths of Ru–Cl(1) 2.4350(11) Å and Ru-Cl(2) 2.4227(11) Å (Table S3†).

In addition, the anthracene moiety and pyridine moiety in 2 are arranged in a head-to-tail aggregation and an offset face-to-face mode, with a distance of 3.6600(4) Å, a shift distance of 1.3413(2) Å , revealing π–π stacking between the anthracene rings in **2** (Fig. 4).

As for compound **2**, the molecular structures are extended into a 3D supramolecular architecture *via* π–π stacking and hydrogen bonds between the Hydrogen atoms on the carbon atoms in the pyridine ring and the coordinated Cl atoms (Table S7† and Fig. 5). Significantly, there is a channel in compound **2** along the *c*-axis (Fig. 6).

Compound **3** crystallizes in the P-1 triclinic space group, and its asymmetric unit consists of one Pt(II) ion, one ADPA ligand, one coordinated chloride ion, and one guest PF_6^- anion (Fig. 7). The Pt(II) center is four coordinated by two N atoms from two pyridine rings, with bond lengths Pt–N(2) 2.0025(3) Å and Pt–N(3) 2.0071(3) Å, one N atom from the amine nitrogen, with a bond length Pt–N(1) 2.0351(3) Å, and one coordinated chloride ion, with a bond length Pt–Cl(1) 2.3064(9) Å (Table S2†).

In **3**, the anthracene moiety and a pyridine moiety, and a pyridine moiety and another pyridine moiety, are arranged in head-to-tail aggregations and an offset face-to-face mode, with distances of 3.5778(1) Å and 3.6886(1) Å, and a shift distance

of 1.4377(29) Å and 1.3566(32) Å, respectively. These facts suggest weak π–π stacking between the aromatic rings in compound **3** (Fig. 8).

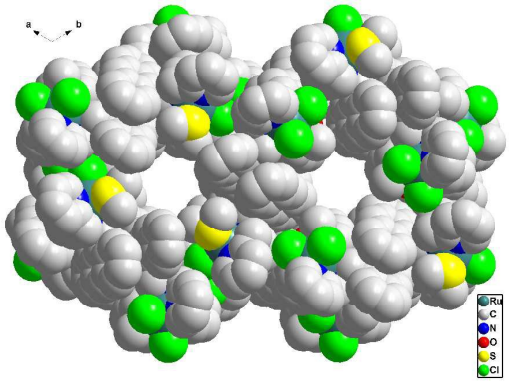

Fig. 6 Channel in 3D supramolecular architecture of 2.

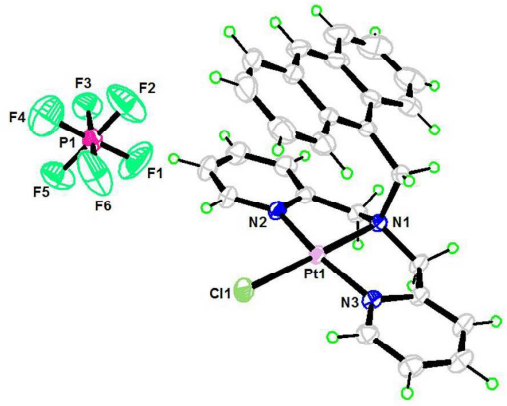

Fig. 7 Molecular structure of **3** with thermal ellipsoids at 45% probability.

There are also intramolecular and intermolecular hydrogen-bonding interactions in **3**. The first type is intramolecular hydrogen bonds between the carbon atoms in the pyridine ring and the Cl(1) atoms [C(16)–H(16A)···Cl(1) = 3.3512 Å, ∠C(16)–H(16A)···Cl(1) = 118° and C(22)–H(22A)···Cl(1) = 3.3177 Å, ∠C(22)–H(22A)···Cl(1) = 118°]. Intramolecular hydrogen bonding enhances the stability of the molecular structure. The second type is intermolecular hydrogen bonds between the carbon atoms in the pyridine ring, Cl atoms, and F atoms in PF_6^- (Table S6†). These π–π stacking and hydrogen-bonding interactions expand the molecular structure into a 3D supramolecular architecture (Fig. 9).

In vitro antimicrobial assay

The *in vitro* antimicrobial activities of ADPA and **1**–**3** against a Gram-positive bacterium (*S. aureus*, CGMCC-1.1477), a Gram-negative bacterium (*E. coli*, ATCC-25922), and a fungus (*C. albicans*, ATCC-10213) were tested. Table 1 shows the MIC (μg/mL) and MBC values (μg/mL). The results show that the compounds showed better activities than the ligand. The increased activity can be attributed to the formation of chelates, which are less polar than the metal elements, and this increases the lipophilicity. The increased lipophilicity of the chelate improves interactions between the compounds and the cell consti nal cell

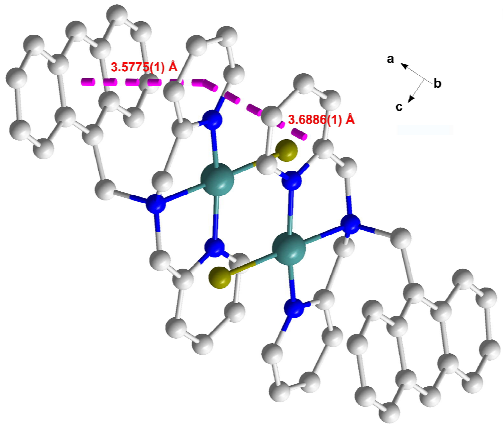

Fig. 8 View of the π-π interaction between aromatic rings in **3**.

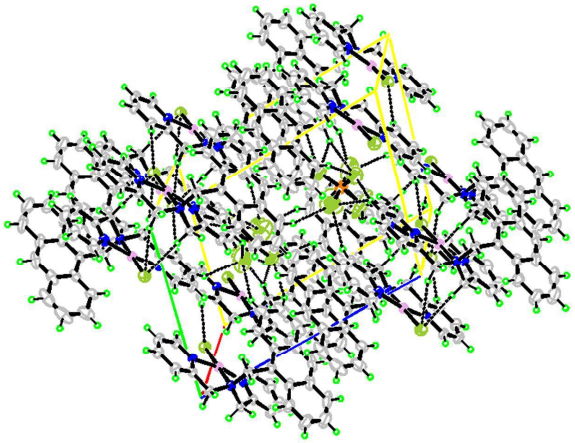

Fig. 9 The hydrogen bond interaction in compound **3** (*c*-axis projection).

Table 1 *In vitro* antimicrobial activities of ADPA and **1**–**3**.

Compounds	*E.coli*		*S.aureus*		*C.albican*	
	MIC[a]	MBC[b]	MIC	MBC	MIC	MBC
ADPA	>1000	>1000	>1000	>1000	>1000	>1000
1	>1000	>1000	156.25	>1000	>1000	>1000
2	>1000	>1000	156.25	312.5	625	>1000
3	>1000	>1000	156.25	300.5	520	>1000

[a]MIC values (μg/mL) – inhibitory activity; [b]MBC values (μg/mL) – microbicidal activity.

processes.[18] Unfortunately, the Gram-negative bacterium (*E. coli*) is insensitive to the ligand and compounds **1**–**3**. The activities of **1**–**3** against the Gram-positive bacterium (*S. aureus*) are higher than those against the fungus (*C. albicans*). Based on the data in Table 1, we concluded that the order of the activities is Pt(II) > Ru(II) > Cu(II). This study, which is part of our efforts to develop new metal-based antimicrobial compounds, shows that the new compounds **2** and **3** may be candidates for treating *S. aureus* and *C. albicans* infections

Conclusions

We designed and successfully synthesized three new Cu(II), Ru(II), and Pt(II) compounds. The crystal structures of the compounds were determined using single-crystal XRD. The single-crystal XRD analysis shows that the three compounds have mononuclear, 0D structures, which are further connected by hydrogen bonds into 3D supramolecular architectures. The synthesized ligand (ADPA) does not have antimicrobial activity, but its Cu(II), Ru(II), and Pt(II) compounds are potential antimicrobial agents against both Gram-positive bacteria (*S. aureus*) and fungi (*C. albicans*). The antimicrobial activities were evaluated based on MIC and MBC values. The potential antimicrobial actions are bacteriostatic and microbicidal. Compounds of **1**–**3**, which exhibit bacteriostatic and microbicidal activities, and especially compounds **2** and **3**, could be developed as new antimicrobial agents for treating *S. aureus* and *C. albicans* infections.

Acknowledgments

This work was supported by the National Natural Science Foundation of China (21172037 and 81360471), the international cooperation project of Guizhou province(No. [2012]7036), and the Natural Science Foundation of Fujian, China (Grant No. 2011J01040) for financial support.

Notes and references

[a] College of Chemistry, Fuzhou University, Fuzhou 350108, China Tel.: +86 591 22866235; fax: +86 591 22866227; e-mail address: jdhuang@fzu.edu.cn (J.-D. Huang).

[b] School of Pharmacy, Zunyi Medical University, Zunyi, Guizhou, 563003,China.Tel.:+86 852 8608579; fax: +86 8528609343;e-mail address: zlyuan2002@126.com.

†Electronic Supplementary Information (ESI) available: Crystallographic information, additional figures, NMR, H RMS,FT-IR, UV-vis, TGA and XRD pattern. CCDC: 1004587 (for **1**), 992195 (for **2**) and 1003395(for **3**). For ESI and crystallographic data in CIF or other electronnic format see DOI: 10.1039/b000000x/.

1 (a) N. V. Lakshmi, P. M. Sivakumar, D. Muralidharan, M. Doble and P. T. Perumal, *RSC Adv*., 2013, **3**, 496.; (b) H. Mohammad, A.S. Mayhoub, A. Ghafoor, M. Soofi, R. A. Alajlouni, M. Cushman and M.N.Seleem, *J. Med. Chem*., 2014, **57**, 1609; (c) S.A. Cochrane, C.T. Lohans, J.R. Brandelli, G. ulvey, G. D. Armstrong and J. C. Vederas, *J. Med. Chem*., 2014, **57**, 1127.

2 (a) G. Jose, T.H.S. Kumara, G. Nagendrappa, H.B.V. Sowmya, J. P. Jasinski, S. P. Millikan, N. Chandrika, S. S. More and B.G. Harish, *Eur. J. Med. Chem.*, 2014, **77**, 288; (b) H. Singh, J. Sindhu, J. M. Khurana, C Sharma, K. R. Aneja, *RSC Adv*., 2014, **4**, 5915.

3 (a) A. F. Elhusseiny and H. H. A. M. Hassan, *Spectrochim. Acta, Part A*., 2013, **103**, 232;(b) B. Una, L. Vesna, V. Vesna, B. Milica, M. Zoran, D. Suzana, *Mater. Lett*., 2014, **128**, 75; (c) N. S. Ng, P. Leverett, D. E. Hibbs, Q.F. Yang, J. C. Bulanadi, M. J. Wu and J. R. Aldrich-Wright, *Dalton Trans*., 2013, **42**, 3196.

4 (a) S. Betanzos-Lara, I. Gracia-Mora, P. Granada-Macías, M. Flores-Álamo and N. Barba-Behrens, *Inorg. Chim. Acta*., 2013, **397**, 94; (b) A. Solanki, S. B. Kumar, A. A. Doshi and C. R. Prabha, *Polyhedron*., 2013, **63** , 147.

5 (a) F. B. Nascimento, G. V. Poelhsitz, F. R. Pavan, D. N. Sato, C. Q. F. Leite, H. S. Selistre-de-Araújo, J. Ellena, E. E. Castellano, V. M. Deflon and A. A. Batista, *J. Inorg. Biochem*., 2008, **102**, 1783; (b) N. S. Shailendra, N. Bharti, M. T. G. Garza, D. E. Cruz-Vega, J. C. Garza, K. Saleem, F. Naqvi and A. Azam, *Bioorg. Med. Chem. Lett*., 2001, **11**, 2675.

6 Q. Wang, Q. M. Feng, H. Lu, W. Q. Wang, Y. Huang and D. Z. Wang, *RSC Adv*., 2013, **3**, 15211.

7 (a) N. Raman and N. Pravi, *Eur. J. Med. Chem.*, 2014, **80**, 57; (b) I. Pradeep, S. Megarajan, S. Arunachalam, R. Dhivya, A. Vinothkanna, M. A. Akbarsha and S. Sekar, *New. J. Chem*., 2014, **38**, 4204; (c) I. Papazoglou, P. J. Cox, A. G. Hatzidimitriou, C. Kokotidou, T. Choli-Papadopoulou and P. Aslanidis, *Eur. J. Med. Chem.*, 2014, **78**, 383; (d) S. Ambika, S. Arunachalam, R. Arun and K. Premkumar, *RSC Adv*., 2013, **3**, 16456.

8 (a) B. Biersack, R. Diestel, C. Jagusch, F. Sasse and R. Schobert, *J. Inorg. Biochem.*, 2009, **103**, 72; (b) M. Galanski and B.K. Keppler, *Pharm. Unserer. Zeit*., 2006, **35**, 118.

9 (a) D. Chatterjee, P. Banerjee, J. C. Bose K and S. Mukhopadhyay, *Dalton Trans*., 2012, **41**, 2694; (b) P. Chellan, K. M. Land, A. Shokar, A. Au, S. H. An, D. Taylor, P. J. Smith, T. Riedel, P. J. Dyson, K. Chibale and G. S. Smit, *Dalton Trans*., 2014, **43**, 513.

10 (a) A. Karaküçük- İyidoğan, D. Taşdemir, E. E. Oruç-Emre and J. Balzarin, *Eur. J. Med. Chem.*, 2011, **46**, 5616; (b) K. Wiglusz and L. Trynda-Lemies, *J. Photochem. Photobi. A.*, 2014, **289**, 1; (c) S. U. Rehman, A.A.Isab, M. N. Tahir, T. Khalid, M. Saleeme, H. Sadaf and S. Ahmad, *Inorg. Chem. Comm.*, 2013, **36**, 68; (d) R. Starosta, A.Bykowska, M. Barys, A.K. Wieliczko, Z. Staroniewicz and J. B. Mał gorzata, *Polyhedron.*, 2011, **30** , 2914.

11 (a) S. Venitt, C. Crofton-Sleigh, M. Agbandje, T. C. Jenkins and S. Neidle, *J. Med. Chem*., 1998, **41**, 3748; (b) O. C. Mansour, B. J. Evison, B. E. Sleebs, K. G. Watson, A. Nudelman, A. Rephaeli, D. P. Buck, J. G. Collins, R. A. Bilardi, D. R. Phillips and S. M. Cutts, *J. Med. Chem*., 2010, **53**, 6851.

12 (a) B. Uttara, K. Imran, H. Akhtar, K. Paturu and R. C. Akhil, *Angew. Chem. Int. Ed.*, 2012, **51**, 2658; (b) H. R. Lucas, G. J. Meyer and K. D. Karlin, *J. Am. Chem. Soc.*, 2009, **131**, 13924.

13 (a) A. Garai, U. Basu, I. Khan, I. Pant, A. Hussain, P. Kondaiah and A. R. Chakravarty, *Polyhedron*, 2014,**73**, 124; (b) G. Canard and C. Pigue, *Inorg. Chem.*, 2007, **46**, 3511; (c) Y. M. Zhao, W. J. He, P. F. Shi, J. H. Zhu, L. Qiu, L. P. Lin and Z. J. Guo, *Dalton Trans.*, 2006, **35**, 2617.

14 CrystalClear, version 1.36, Molecular Structure Corp and Rigaku Corp., The Woodlands, TX, and Tokyo, Japan, 2000.

15 G. M. Sheldrick, SHELXS 97, Program for Crystal Structure Solution; University of Göttingen: Göttingen, Germany.

16 (a) S. D. Sarker, L. Nahar and Y. Kumarasamy, *Methods.*, 2007, **42**, 321; (b) Z. L. Yuan, Q. H. Hu, Q. Wu, M. Q. Zhang and B. X. Zhu, *Chin. J. Org. Chem.*, 2009, **29**, 279; (c) A. Bolmströ, *Diagn. Micr. Infec. Dis.*, 1994, **19**, 187; (d) G. S. Hall, K. Pratt-Rippin, D. M. Meisler, J. A. Washington, T. J. Roussel and D. Miller, *Diagn. Micr. Infec. Dis.*, 1995, **21**, 187; (e) D. C. Ilies, E. Pahontu, S. Shova, R. Georgescu, N. Stanica, R.Olar, A. Gulea and T. Rosu, *Polyhedron.*, 2014, **81**, 123; (f) Z.

L. Yuan, Q. Wu, X. B. Yang, Q. H. Hu and M. Q. Zhang, *Chin. J. Org. Chem.*, 2011, **31**,1698; (g) L. Motiei, S. Rahimipour, D. A. Thayer, C.H. Wong and M. R. Ghadiri, *Chem. Commun.*, 2009, **45**, 3693.

17 Z. L.Yuan, X. Q. Yang, L. Wang, J. D. Huang and G. Wei, *RSC Adv*., 2014, **4**,42211.

18 H. H. Liu, W. Yang, W. Q. Zhou, Y .L. Xu, J. Xie, M. Y. Li, *Inorg. Chim. Acta.*, 2013, **405**, 387 .

19 (a) J. Mola, I. Romero, M. Rodríguez, F. Bozoglian, A. Poater, M. Solà, T. Parella, J. Benet-Buchholz, X. Fontrodona and A. Llobet, *Inorg. Chem*., 2007, **46**, 10707; (b) A. M. S. Silva, J. A. S. Cavaleiro, G. Tarrago and C. Marzin, *New J. Chem*., 1999, **23**, 329; (c) I. Bratsos, E. Mitri, F. Ravalico, E. Zangrando, T. Gianferrara, A. Bergamo and E. Alessio, *Dalton Trans*., 2012, **41**, 7358.

20 (a) L. A. Mullice, R. H. Laye, L. P. Harding, N. J. Buurma and S. J. A. Pope, *New J. Chem*., 2008, **32**, 2140; (b)Y. M. Zhao, W.J. He, S. Pengfei, J. H. Zhu, L. Qiu, L. P. Lin and Z. J. Guo, *Dalton Trans*., 2006, **22**, 2617;(c) I. Bratsos, S. Calmo, E. Zangrando, G. Balducci, and E. Alessio, *Inorg. Chem.*, 2013, **52**, 12120.

21 (a)J. H. Price, A. N. Williamson, R. F. Schramm and B. B.Wayland, *Inorg. Chem.*,1972, **11**, 1280; (b) R. M. Dyksterhouse, B. A. Howell and P. J. Squattrito, *Acta Crystallogr.*, 2000, **C56**, 64; (c) P. Bitha, G. O. Morton, T. S. Dunne, E. F. Delos Santos, Y. Lin, S. R. Boone, R. C. Haltiwanger and C. G. Pierpont, *Inorg. Chem.*, 1990, **29**, 645.

22 R. Romeo, S. Lanza, M. L. Tobe, *Inorg. Chem.*, 1977, **16**, 785.

23 M. T. Forel, M. Tranquille, *Spectrochim. Acta.*, 1970, **26A**, 1023.

24 (a)D. Kovala-Demertzi, M. A. Demertzis, J. R.Miller, C. S. Frampton, J. P. Jasinski, D. X. West, *J. Inorg. Biochem.*, 2002, **92**, 137; (b) Z.L.Yuan, Q. L. Zhang, X. Liang, B. X. Zhu, L. F. Lindoy and G. Wei, *Polyhedron*., 2008, **27**, 344; (c) P. Singh, D. P. Singh and V. P. Sing, *Polyhedron*., 2014, **81**, 56; (d) J. Z. Zhao, S. M. Ji, W. H. Wu, W. T. Wu, H. M. Guo, J. F. Sun, H. Y. Sun, Y. F. Liu, Q. T. Li and L. Huang, R*SC Adv.*, 2012, **2**, 1712.

25 (a) H.J. Lv, J. A. Rudd, P. F. Zhuk, J.Y. Lee, E. C. Constable, C. E. Housecroft, C. L. Hill, D. G. Musaev and Y. V. Geleti, *RSC Adv*., 2013, **3**, 20647; (b) H.H.Liu, W.Yang, W.Q. Zhou, Y.L. Xu, J. Xie and M.Y. Li, *Inorg. Chim. Acta*., 2013, **405**, 387; (c) E. C. Constable and A. M. W. C. Thompson, *Dalton Trans.*, 1994, **9**, 1409.

26 M. Wrighton and D. L. Morse, *J. Am. Chem. Soc*., 1974, **96**, 998.

27 Q. P. Li, C. B. Tian, H.B. Zhang, J. J. Qian and S.W. Du, *CrystEngComm***.**, 2014, **16**, 9208.

